

Article

Characterization and Identification of Prenylated Flavonoids from *Artocarpus heterophyllus* Lam. Roots by Quadrupole Time-Of-Flight and Linear Trap Quadrupole Orbitrap Mass Spectrometry

Jin-Bao Ye ^{1,*}, Gang Ren ^{1,*} , Wen-Yan Li ¹, Guo-Yue Zhong ¹, Min Zhang ², Jin-Bin Yuan ^{2,*} and Ting Lu ¹

¹ Research Center of Natural Resources of Chinese Medicinal Materials and Ethnic Medicine, Jiangxi University of Traditional Chinese Medicine, Nanchang 330004, China; 201781800024@jxutcm.edu.cn (J.-B.Y.); liwenyan369@126.com (W.-Y.L.); zgy1037@163.com (G.-Y.Z.); 18770839821@163.com (T.L.)

² Key Laboratory of Modern Preparation of TCM, Ministry of Education, Jiangxi University of Traditional Chinese Medicine, Nanchang 330004, China; zfishm@163.com

* Correspondence: 20091005@jxutcm.edu.cn (G.R.); kings2008@163.com (J.-B.Y.)

Academic Editor: Gerold Jerz

Received: 19 November 2019; Accepted: 11 December 2019; Published: 15 December 2019



Abstract: In this study, a combination of quadrupole time-of-flight mass spectrometry (Q-TOF-MS) and linear trap quadrupole orbitrap mass spectrometry (LTQ-Orbitrap-MS) was performed to investigate the fragmentation behaviors of prenylated flavonoids (PFs) from *Artocarpus* plants. Fifteen PFs were selected as the model molecules and divided into five types (groups A–E) according to their structural characteristics in terms of the position and existing form of prenyl substitution in the flavone skeleton. The LTQ-Orbitrap-MSⁿ spectra of the [M – H][–] ions for these compounds provided a wealth of structural information on the five different types of compounds. The main fragmentation pathways of group A were the ortho effect and retro Diels–Alder (RDA), and common losses of C₄H₁₀, CO, and CO₂. The compounds in group B easily lose C₆H₁₂, forming a stable structure of a 1,4-dienyl group, unlike those in group A. The fragmentation pathway for group C is characterized by obvious ^{1,4}A[–], ^{1,4}B[–] cracking of the C ring. The diagnostic fragmentation for group D is obvious RDA cracking of the C ring and the successive loss of CH₃ and H₂O in the LTQ-Orbitrap-MSⁿ spectra. Fragmentation with successive loss of CO or CO₂, ·CH₃, and CH₄ in the LTQ-Orbitrap-MSⁿ spectra formed the characteristics of group E. The summarized fragmentation rules were successfully exploited to identify PFs from *Artocarpus heterophyllus*, a well-known *Artocarpus* plant, which led to the identification of a total of 47 PFs in this plant.

Keywords: prenylated flavonoids; *Artocarpus heterophyllus*; Q-TOF-MS; LTQ-Orbitrap-MS; fragmentation rules; identification

1. Introduction

Prenylated flavonoids (PFs) are a class of structurally distinct chromone derivatives characterized by several prenyl units linked to a flavone nucleus by C–C and/or C–O bonds. PFs possess high structural diversity due to various prenyl substitution patterns on the flavone skeleton, which correspond to their wide range of biological activities such as cytotoxicity [1], tyrosinase inhibition [2], and cathepsin K inhibition [3,4], as well as antiplasmodial [5], antitypanosomal [5], and anti-inflammatory [6] activity, and inhibition of neutrophil respiratory burst [7]. Due to their complex chemical diversity and wide range of biological activities, the search for structurally interesting and biologically active PFs from natural products has attracted the intense attention of natural product chemists and

pharmacologists in the past few decades. Interestingly, the occurrence of PFs appears to have a significantly chemotaxonomical tendency and is limited to within only a few plant families, including Moraceae. The genus *Artocarpus* of Moraceae has been reported as a rich source of PFs, and more than 300 have been isolated from *Artocarpus* plants to date [8,9].

Artocarpus heterophyllus Lam., a well-known member of *Artocarpus*, is an evergreen arbor widely distributed in tropical and subtropical regions of Asia, such as Thailand, Vietnam, the Philippines, and other countries [10]. In China, *A. heterophyllus* is popularly cultivated for its popular edible fruits, while its root has been used in folk medicine for subduing swelling and detoxicating [11]. A variety of bioactive PFs were previously identified from *A. heterophyllus* using the conventional process of isolation and purification on a preparative scale followed by structure elucidation via spectroscopic methods [4,12,13]. However, the purification of PFs from the crude extract by this conventional method is usually time-consuming, tedious, and labor-intensive due to their thermal sensitivity and low abundance in *A. heterophyllus*.

The combination of quadrupole time-of-flight mass spectrometry (Q-TOF-MS) and linear trap quadrupole orbitrap mass spectrometry (LTQ-Orbitrap-MS) is a powerful analytical strategy to rapidly screen and identify trace compounds. The combined method possesses high resolution, high mass accuracy, high sensitivity, and abundance fragment information. It is frequently used for the structural characterization of natural products in crude extracts, especially when the reference compounds are unavailable [14–16]. Despite there being vast numbers of known PFs, their fragmentation behaviors and corresponding mechanisms remain relatively unexplored.

In the present work, 15 PFs previously isolated and identified [17–20] from the extract of *Artocarpus* plants were selected as model molecules and divided into five types according to the substitution pattern of prenylated groups in the flavone nucleus. The fragmentation behaviors of all the five types of PFs were systematically investigated by Q-TOF-MS and LTQ-Orbitrap-MSⁿ. Based on these summarized fragmentation rules, a total of 47 trace PFs were identified. In this work we developed an effective mass spectrometric method for the rapid identification of PFs in mixtures; this could also provide a valuable aid for the characterization of PFs in other PF-containing medicinal herbs.

2. Results and Discussion

The chemical structures of the 15 reference PFs are shown in Figure 1. According to the positions and existence of prenylated substitution in the flavone skeleton, these compounds fall into five categories: group A: free 6- or 8-prenylated substituted flavones (PFs 1–3); group B: free 8-geranyl substituted flavones (PFs 4 and 5); group C: free 3-prenylated substituted flavones (PFs 6–9); group D: 3-partial heterocyclization-prenoid substituted flavones (PFs 10 and 11); and group E: dihydrobenzoxanthone derivatives (PFs 12–15).

All the investigated reference compounds were initially analyzed by electrospray ionization quadrupole time-of-flight (ESI-Q-TOF) mass spectrometry in both positive and negative ion modes. Each group of PFs exhibited a strong molecular ion peak ($[M - H]^-$ in negative ion mode) with a very small percentage of fragments in the Q-TOF-MS spectrum, and yielded a wealth of product ions in the subsequent TOF-MS/MS and LTQ-Orbitrap-MSⁿ spectra. Accordingly, the $[M - H]^-$ ions were selected as the precursor ions for collision-induced dissociation (CID) fragmentation to produce MS/MS spectra, and the relatively prominent product ions were then chosen for further MSⁿ analysis. As summarized in Table 1, these MSⁿ spectra provided abundant fragment ions for the structural characterization and identification of PFs. Using this rule, a total of 47 PFs in the extract of the *A. heterophyllus* were rapidly identified by ultra-high performance liquid chromatography (UPLC)-Q-TOF-MS/MS.

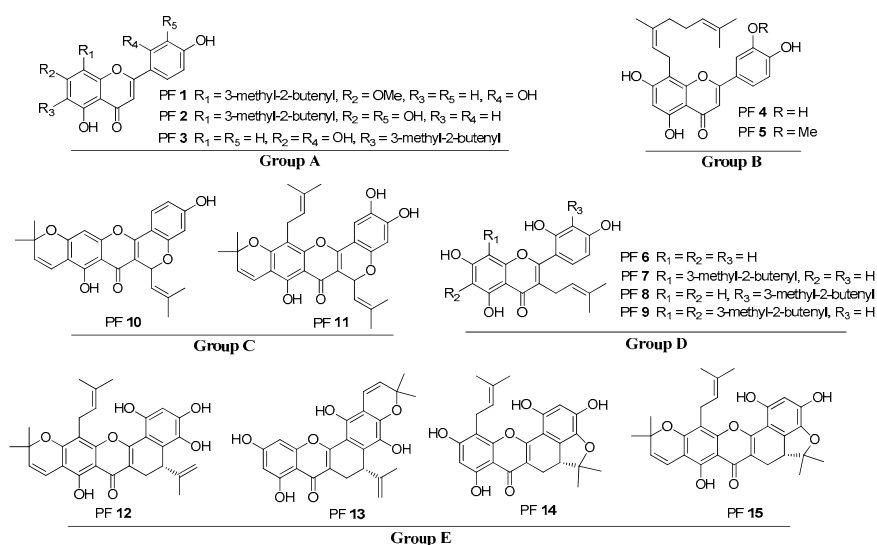


Figure 1. Structures of the five groups of prenylated flavonoids (PFs) selected as model molecules from *Artocarpus* plants.

Table 1. Precursor ions and main product ions observed in the electrospray ionization quadrupole time-of-flight mass spectrometry (ESI-Q-TOF-MSⁿ) and linear trap quadrupole orbitrap mass spectrometry (LTQ-Orbitrap-MSⁿ) spectra of the protonated PFs 1–15.

Compounds	MS ⁿ	Precursor Ions	Product Ions <i>m/z</i> (Relative Abundance, %)
PF 1	MS/MS	367 [M – H] [–]	175 (3.4); 233 (3.9); 265 (4.2); 297 (18.9); 309 (77.7); 337 (1.6); 352 (1.7); 367 (100.0)
	MS ³	233	133 (20.4); 165 (61.7); 189 (23.7); 217 (100.0)
		309	175 (61.7); 265 (100.0); 291 (26.7)
PF 2	MS ⁴	265	173 (100.0); 193 (36.4); 215 (62.1); 221 (75.1); 237 (70.1)
	MS/MS	353 [M – H] [–]	133 (6.8); 297 (15.5); 309 (15.5); 353 (100.0)
	MS ³	297	225 (20.1); 227 (21.4); 253 (97.5); 255 (83.4); 269 (100.0)
		309	265 (18.8); 267 (19.9); 309 (100.0)
PF 3	MS ⁴	269	225 (53.4); 227 (35.2); 241 (75.7); 251 (100.0); 269 (39.3)
	MS/MS	353 [M – H] [–]	211 (10.4); 223 (17.9); 239 (44.7); 252 (20.5); 267 (100.0)
	MS ³	219	133 (2.0); 219 (9.8); 309 (3.1); 353 (100.0)
PF 4	MS ⁴	175	65 (13.4); 133 (100.0)
	MS/MS	421 [M – H] [–]	133 (12.7); 161 (8.9); 255 (9.4); 269 (8.7); 297 (100.0); 323 (12.4); 337 (12.0); 421 (21.9)
	MS ³	297	163 (9.8); 225 (22.8); 227 (22.1); 253 (100.0); 255 (84.4); 269 (95.9)
PF 5	MS ⁴	253	211 (10.7); 225 (100.0); 253 (22.9)
	MS/MS	435 [M – H] [–]	133 (6.7); 269 (8.); 297 (84.5); 309 (30.1); 311 (13.5); 323 (21.1); 351 (100.0); 420 (35.4); 435 (32.8)
	MS ³	297	163 (9.0); 225 (20.9); 227 (21.0); 253 (88.6); 255 (75.6); 269 (100.0)
PF 6	MS ⁴	351	307 (9.2); 309 (19.1); 333 (24.0); 351 (100.0)
		253	211 (8.38); 225 (100.0); 253 (20.2)
	MS/MS	353 [M – H] [–]	109 (16.7); 125 (30.6); 151 (24.8); 231 (100.0); 243 (13.2); 283 (11.6); 284 (62.0); 353 (50.5)
	MS ³	231	145 (23.1); 147 (23.2); 149 (24.0); 151 (76.7); 163 (23.0); 187 (100.0); 189 (28.2)
MS ⁴	284	256 (100.0)	
	256	122 (100.0); 212 (56.7); 227 (43.6); 228 (38.3)	

Table 1. Cont.

Compounds	MS ⁿ	Precursor Ions	Product Ions <i>m/z</i> (Relative Abundance, %)
PF 7	MS/MS	421 [M – H] [–]	193 (8.91); 219 (1.9); 227 (1.8); 283 (2.4); 297 (7.7); 299 (20.9); 309 (38.8); 311 (3.1); 421 (100.0)
	MS ³	193	125 (43.1); 149 (100.0); 151 (36.2)
		309	175 (92.2); 265 (100.0)
	MS ⁴	149	107 (100.0)
		265	173 (59.8); 175 (44.4); 215 (74.5); 221 (76.7); 223 (100.0); 237 (56.2)
PF 8	MS/MS	421 [M – H] [–]	193 (7.1); 293 (7.7); 299 (27.7); 309 (47.1); 421 (100.0)
	MS ³	299	244 (90.0)
		309	175 (10.2); 244 (100.0); 256 (19.7); 299 (78.7)
	MS ⁴	299	244 (100.0); 299 (58.0)
		244	123 (100.0); 149 (35.3); 150 (69.0); 203 (53.3); 215 (35.8); 216 (77.4); 229 (99.11)
PF 9	MS/MS	489 [M – H] [–]	261 (6.1); 351 (6.0); 365 (10.3); 367 (100.0); 377 (75.9); 489 (90.4)
	MS ³	367	257 (10.6); 269 (24.5); 312 (100.0); 367 (71.2)
		377	269 (10.1); 312 (31.5); 367 (100.0)
	MS ⁴	312	257 (51.4); 269 (100.0)
PF 10	MS/MS	417 [M – H] [–]	199 (2.3); 217 (3.0); 333 (7.3); 347 (2.4); 361 (11.7); 373 (6.29); 387 (2.8); 401 (3.3)
	MS ³	361	319 (7.5); 334 (13.5); 343 (100.0); 346 (59.4)
	MS ⁴	343	199 (22.1); 287 (36.2); 299 (10.0); 315 (24.2); 343 (100.0)
PF 11	MS/MS	501 [M – H] [–]	285 (3.8); 429 (3.7); 457 (43.22); 473 (3.3); 501 (100.0)
	MS ³	285	285 (5.2); 243 (22.0); 241 (100.0); 217 (8.5)
		457	402 (20.1); 439 (100.0); 442 (10); 457 (18.7)
		241	133 (67.5); 157 (32.2); 173 (77.2); 193 (26.6); 197 (100.0); 213 (32.5)
	MS ⁴	439	357 (58.70); 383 (21.73); 395 (53.51); 411 (100.0); 424 (20.26)
		411	329 (35.9); 341 (87.8); 354 (73.8); 356 (87.3); 367 (54.4); 383 (76.9); 393 (58.3); 396 (100.0); 411 (22.5)
PF 12	MS/MS	501 [M – H] [–]	415 (8); 417 (5.0); 429 (7.3); 445 (14.8); 457 (4.2); 471 (13.0); 483 (4.4); 501 (100.0)
	MS ³	445	355 (25.3); 373 (38.8); 399 (39.0); 403 (26.7); 417 (100.0); 427 (94.2); 445 (74.6)
		485	429 (100.0); 442 (60.3); 457 (29.9); 469 (46.5); 471 (85.7)
	MS ⁴	427	355 (53.9); 383 (10.5); 399 (100.0); 427 (34.5)
		429	401 (100.0); 411 (31.5); 414 (20.5)
	MS ⁵	399	343 (52.5); 355 (100.0); 356 (41.6)
		401	357 (88.5); 373 (100.0); 383 (26.6); 386 (70.6); 401 (19.3)
PF 13	MS/MS	433 [M – H] [–]	373 (11.3); 389 (37.0); 390 (63.2); 405 (25.3); 417 (11.2); 433 (100.0)
	MS ³	389	361 (15.2); 372 (100.0); 373 (34.3); 375 (17.5); 389 (27.9)
		405	335 (17.4); 350 (32.9); 361 (27.9); 360 (30.4); 372 (21.9); 389 (15.1); 405 (100.0)
	MS ⁴	372	326 (34.9); 327 (35.9); 343 (71.7); 371 (100.0)
		350	309 (21.6); 335 (100.0); 349 (22.2)
	MS ⁵	343	299 (13.9); 343 (100.0)
		335	276 (16.0); 291 (68.1); 308 (25.6); 317 (34.2); 335 (100.0)
	MS ⁶	299	263 (14.0); 276 (100.0); 291 (16.7)
		291	263 (14.0); 276 (100.0); 291 (16.7)
	PF 14	MS/MS	435 [M – H] [–]
MS ³		349	277 (21.4); 305 (15.0); 321 (32.9); 349 (100.0)
		391	337 (29.5); 349 (100.0); 363 (23.9); 377 (17.8)
MS ⁴		321	264 (100.0); 276 (40.7); 279 (62.5); 293 (90.0)
		337	309 (100.0)
MS ⁵		309	237 (21.1); 263 (32.6); 365 (23.3); 279 (27.0); 281 (70.3); 291 (100.0); 309 (31.4)

Table 1. Cont.

Compounds	MS ⁿ	Precursor Ions	Product Ions <i>m/z</i> (Relative Abundance, %)
PF 15	MS/MS	501 [M – H] [–]	417 (5.0); 429 (5.5); 443 (5.8); 445 (12.2); 457 (7.3); 471 (7.7); 485 (14.8); 501 (100.0)
	MS ³	445	355 (27.4); 373 (41.3); 399 (38.9); 417 (99.6); 427 (100.0); 445 (80.8)
		485	429 (100.0); 442 (60.8); 457 (34.2); 469 (47.9); 471 (88.0)
	MS ⁴	427	355 (26.4); 371 (56.0); 385 (27.2); 399 (100.0)
		429	357 (26.3); 374 (19.6); 401 (100.0); 411 (29.9)
MS ⁵	399	355 (100.0); 384 (18.3)	
		401	357 (91.0); 373 (100.0); 383 (32.7); 385 (48.8); 401 (21.8)

2.1. Fragment Naming Rules

In this study, the C–C bond cleavages of different groups occurred at different positions of the C ring. In general, the fragment ions formed by the C–C bond cleavage on the C ring of flavonoids are named ^{ij}A and ^{ij}B [21], where A and B represent benzene ring A and benzene ring B, respectively, on the parent nucleus of the flavonoid. “i” and “j” represent the fracture position of the C–C bond cleavage on the C ring, as shown in Figure 2.

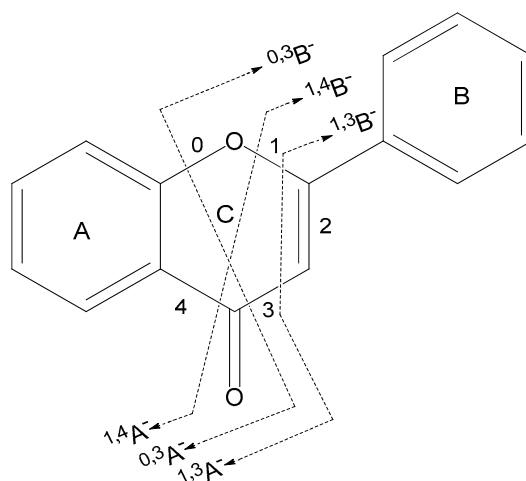


Figure 2. Nomenclature of the different C ring cleavages [21] occurring in the present study, illustrated by a typical flavonoid skeleton.

2.2. Fragmentation of PFs 1–3

PFs 1–3 in group A represent a type of general prenylated flavones with coplanar structure and bearing a free prenyl moiety at the C-6- or -8 position. PFs 1–3 mainly showed the neutral loss of C₄H₈ or C₅H₁₀ via the ortho effect at the C-8 position to yield a prominent ion at *m/z* 297. This fragmentation pathway was found for the first time in PFs. In addition, the product ions ^{1,3}A[–] and/or ^{1,3}B[–] could be deduced, and their fragmentation pathway was retro-Diels–Alder (RDA) cleavage from the 1,3-position of the C-ring. Common losses of other neutral molecules, such as C₄H₁₀, CO, and CO₂, were also observed.

PF 1 was selected as an example to illustrate the fragmentation characteristics of group A. Figure 3, Figures S1–S5 exhibits the typical ESI-MS spectra and fragmentation pathways of PF 1 in negative ion mode by Q-TOF-MS/MS and LTQ-Orbitrap MSⁿ (*n* = 2–4) (Supplementary Materials). The Q-TOF-MS spectrum (Figure 3A) of PF 1 showed a precursor [M – H][–] ion at *m/z* 367.1205 (error 4.90 ppm). In the Q-TOF-MS/MS spectrum (Figure 3B), the prominent ion at *m/z* 297.0412 ([M – H – C₅H₁₀][–], error 2.36 ppm) was from the loss of C₅H₁₀ via the ortho effect at the C-8 position, and the fragmentation at *m/z* 309.0417 ([M – H – C₄H₁₀][–], error 3.88 ppm) was from the loss of C₄H₁₀ at the same position.

Simultaneously, a minor ion at m/z 233.0852 was also detected, owing to RDA fragmentation at the 1,3-position of the C-ring. As shown in Figure 3C, further loss of CO_2 from the ion at m/z 233.0852 generated the product ion at m/z 189.0938 in the LTQ-Orbitrap- MS^3 spectrum. As seen from the MS^{3-4} spectra (Figure 3D,E), a fragment ion at m/z 309.0417 was observed with the initial loss of the CO_2 group at the C ring; subsequently, loss of the CO group at the B ring position yielded prominent ions at m/z 265.0599 $[\text{M} - \text{H} - \text{C}_4\text{H}_{10} - \text{CO}_2]^-$ and m/z 237.0466 $[\text{M} - \text{H} - \text{C}_4\text{H}_{10} - \text{CO}_2 - \text{CO}]^-$. In addition, the fragment ion at m/z 175.0082 from m/z 309.0417 via the classical RDA cleavage pathway was also observed. Figure 3F summarizes the above fragmentation pathway of PF 1.

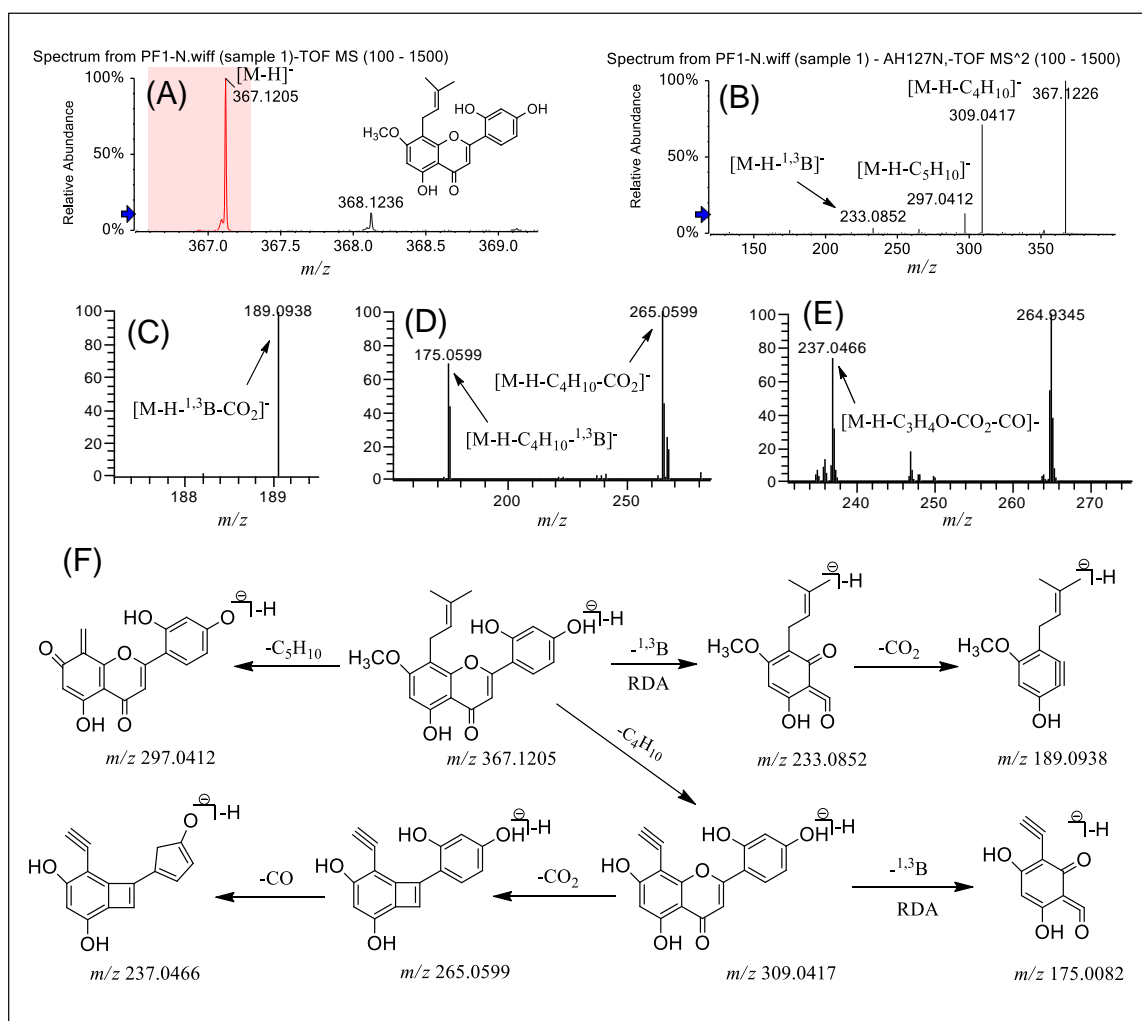


Figure 3. (–) ESI-Q-TOF-MS/MS and LTQ-Orbitrap- MS^n ($n = 3-4$) spectra of PF 1 in group A and the fragmentation pathways proposed for PF 1. Q-TOF-MS (A), Q-TOF- MS^2 (B), LTQ-Orbitrap- MS^3 of the ions at m/z 233.0852 from m/z 367.1205 (C), LTQ-Orbitrap- MS^3 of the ions at m/z 309.0417 from m/z 367.1205 (D), LTQ-Orbitrap- MS^4 of the ions at m/z 265.0599 from m/z 309.0417 (E), and the proposed fragmentation pathways for PF 1 (F). RDA: retro Diels–Alder.

The fragmentation pathways of PFs 1–3 are almost identical, which is in full support of the structural characterization of this type of PF. The characteristic fragment ions described above can be regarded as the important information for the qualification of group A. There are still some differences in the cleavage pathways of the prenyl moieties at C-6 (PF 3) and C-8 (PFs 1 and 2). The fragment ions of PF 3 are relatively few, and the ortho effect was not observed. PF 3 exhibited RDA cleavage at the C-6 position, resulting in a prominent ion at m/z 219.0673 ($[\text{M} - \text{H} - ^{1,3}\text{B}]^-$, error 4.57 ppm) and a fragment ion at m/z 133.0230 ($[\text{M} - \text{H} - ^{1,3}\text{A}]^-$, error 3.76 ppm). However, only one fragment ion appeared via

RDA cleavage for PFs **1** and **2**. These features could help us to differentiate the compounds bearing a free prenyd moiety at the C-6 position from those bearing the same at the C-8 position.

2.3. Fragmentation of PFs **4** and **5**

A detailed comparison revealed that the flavones in groups B and A exhibited much structural similarity. The structural difference lies in the side chains at the C-8 position: geranyl for group B, and prenyl for group A. Compared with the fragmentation behavior of group A, the ortho effect and RDA cleavage in group B exhibited similar characteristics. The difference is that the geranyl group of group B easily loses C₆H₁₂, forming a stable structure of a 1,4 dienyl group.

PF **4** was selected as an example to illustrate the fragmentation pathways of this class of compounds. Figure 4, Figures S20–S24 shows the typical ESI-MS spectra and fragmentation pathways of PF **4** in negative ion mode by Q-TOF-MS/MS and LTQ-Orbitrap-MSⁿ ($n = 2-4$). Q-TOF-MS (Figure 4A) of PF **4** gave a precursor [M – H][–] ion at m/z 421.1644 (error 3.09 ppm). In the Q-TOF-MS/MS spectrum, Figure 4B shows that the prominent ion at m/z 297.0395 ([M – H – C₉H₁₆][–], error 3.37 ppm) could be attributed to the loss of C₉H₁₆ from the precursor at m/z 421.1644 via the ortho effect. The precursor at m/z 421.1644 is able to experience RDA cleavage to form m/z 133.0301 ([M – H – ^{1,3}A][–], error 4.51 ppm), similarly to group A. In comparison with group A, owing to the presence of the geranyl (instead of prenyl) side chain at the C-8 position, group B shows obvious cleavage of the geranyl group and thus loses a C₆H₁₂ group. This tendency is more obvious when there is a methoxy group in the mother nucleus, such as in PF **5**. Figure 4C,D shows the successive loss of CO₂ and CO groups at the C ring, yielding a prominent ion at m/z 225.0474 [M – H – C₉H₁₆ – CO₂ – CO][–] from m/z 297.0395. In addition, the primary daughter ion [M – H – C₉H₁₆ – CO][–] was observed owing to the loss of CO from the product ion at m/z 297.0395. The fragmentation patterns of PF **5** are almost identical to those of PF **4**, in full support of the structural characterization of this type of flavone. Figure 4E summarizes the fragmentation pathways to help identify these compounds, taking PF **4** as an example.

2.4. Fragmentation of PFs **6–9**

Group C contains four free 3-prenylated substituted flavones, with three of them bearing another one or more prenyl moieties at the C-6, -8, and -3' positions, but not PF **6**. For these PFs in group C, non-coplanarity is the common structural feature and results from the free 3-prenylated group in the flavone nucleus forcing the 2-phenyl group out of plane with the chromone ring. This unique stereo configuration of the free 3-prenylated substituted flavones in group C leads to significantly different fragmentation behaviors from the other four groups. The most prominent difference between group C and the other groups is in the fragmentation of the C ring. The C ring of this kind of compound shows obvious ^{1,4}A[–], ^{1,4}B[–] cracking, while the common flavonoids show RDA cracking (^{1,3}A[–], ^{1,3}B[–]).

As shown in Figure 5, Figures S30–S35 PF **6** was taken as an example to illustrate the typical cleavage pathways. Figure 5A shows the molecular ion ([M – H][–], m/z 353.1028, error 0.79 ppm) corresponding to the molecular formula C₂₆H₂₈O₆. The product ions [M – H – B^{1,4}][–] at m/z 125.0242 (error 1.60 ppm) and [M – H – A^{1,4}][–] at m/z 231.1021 (error 2.60 ppm) were from the cracking of the C ring (Figure 5B). The other three compounds all have a similar fragmentation pathway. This kind of cracking was observed only in group C, and not in the other four groups.

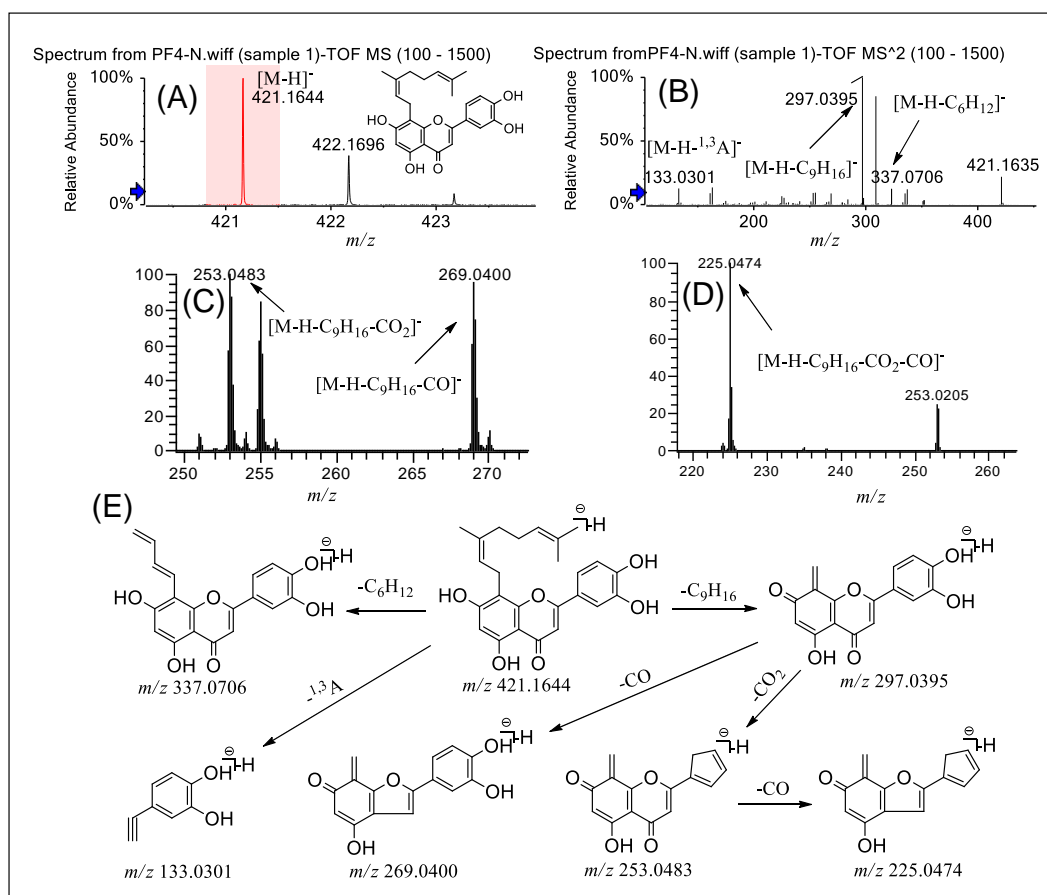


Figure 4. (–) ESI-Q-TOF-MS/MS and LTQ-Orbitrap-MSⁿ ($n = 3–4$) spectra of PF 4 in group B and the fragmentation pathways proposed for PF 4. Q-TOF-MS (A), Q-TOF-MS² (B), LTQ-Orbitrap-MS³ of the ions at m/z 297.0395 from m/z 421.1644 (C), LTQ-Orbitrap-MS⁴ of the ions at m/z 253.0483 from m/z 297.0395 (D), and the proposed fragmentation pathways for PF 4 (E).

PF 6 exhibited a prominent product ion ($[M - H - C_5H_9]^-$, m/z 284.0326, error 0 ppm) which was from the loss of C_5H_9 from the precursor ion (Figure 5B). In addition, the strong product ion peak at m/z 151.0038 ($[M - H - ^{1,3}B]^-$, error 0.62 ppm) was easily obtained via RDA cleavage from the precursor $[M - H]^-$. PF 7 has the same cleavage pathway with a very weak peak ($[M - H - ^{1,3}B]^-$), but PFs 8 and 9 do not have this fragmentation pathway. This characteristic fragmentation pathway can be used to explore the position and number of prenylated groups of these compounds.

Remarkably, these observations indicated that PFs 7–9 are apt to lose the C_4H_8 group at the free 3-prenylated group, forming a stable furan ring closed with the hydroxyl at the C-2' position, and to successively eliminate a C_4H_8 group at the C-8 position, forming a double bond between C-7 and C-8 via the ortho effect. Taking PF 8 as an example, this cracking pathway eventually produced a prominent ion at m/z 309.0432 ($[M - H - C_8H_{16}]^-$, error 3.88 ppm). The characteristic fragmentation pathway of group C is of great significance for the identification of these compounds containing more than two prenyl groups.

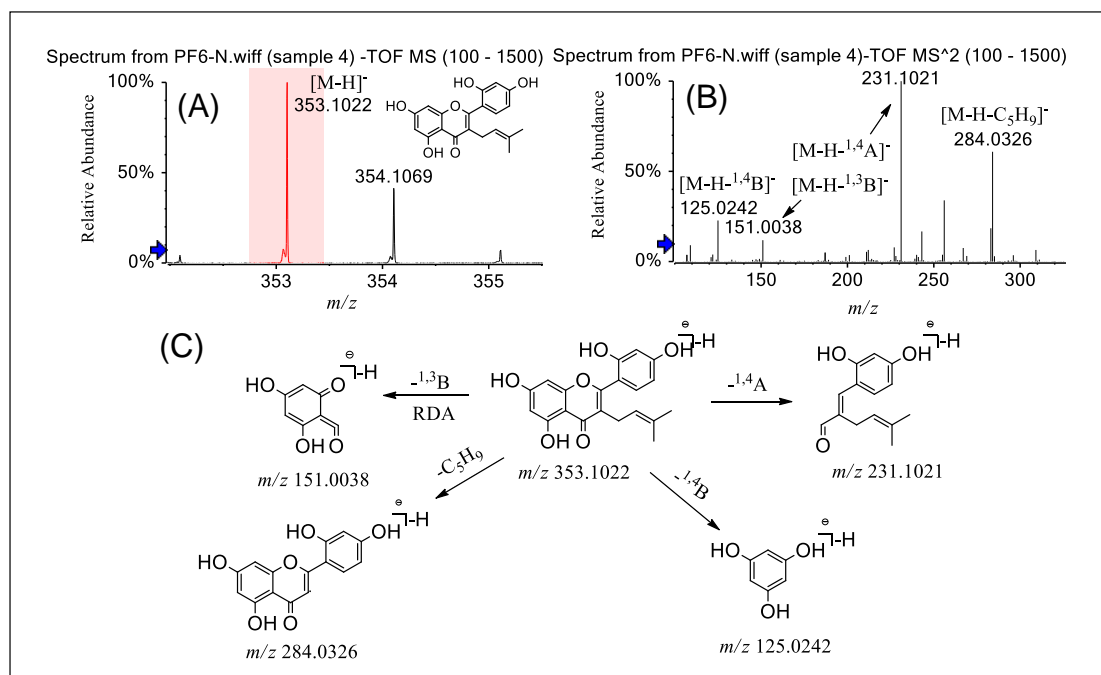


Figure 5. (–)ESI-Q-TOF-MS/MS of PF 6 in group C and the fragmentation pathways proposed for PF 6. Q-TOF-MS (A), Q-TOF-MS² (B), and the proposed fragmentation pathways for PF 6 (C). RDA: retro Diels–Alder.

2.5. Fragmentation of PFs 10 and 11

The two compounds in group D are also 3-prenylated flavones similar to those in group C, but they possess a coplanar structure in which the prenyl substituent at the 3-position is partially heterocyclized to form a pyran ring by C–O linkage between C-11 of the prenylated moiety and the hydroxyl group at the C-2' position of the B ring. The existence of the C-11/C-2' pyran ring in group D resulted in a wealth of product ions in the MSⁿ ($n = 2–5$) spectra, which is notably different from group C. The most significant difference between group D and C is the cracking behavior of the C ring: RDA cleavage mainly occurred in group D, and ^{1,4}A[–]/^{1,4}B[–] cracking occurred in group C. The difference could be used to differentiate the two groups.

PF 10 was selected as an example to illustrate the fragmentation pathways of group D. Figure 6, Figures S51–S56 exhibits the typical ESI-MS spectra and fragmentation pathways of PF 10 in negative ion mode by Q-TOF-MS/MS and LTQ-Orbitrap-MSⁿ ($n = 2–4$). The mass spectrum of PF 10 in Figure 6A showed a precursor ion [M – H][–] at m/z 417.1358 ([M – H][–], error 3.41 ppm). PF 10 is mainly cracked via RDA, producing the fragment ions at m/z 217.0516 ([M – H – ^{1,3}B][–]) in the Q-TOF-MS/MS spectrum (Figure 6B). In addition, the fragment ion at m/z 361.0737 ([M – H – 4·CH₃][–], error 3.60 ppm) came from the loss of ·CH₃ from the precursor ion [M–H][–]. In the LTQ-Orbitrap-MS^{3–4} spectra of PF 10 (Figure 6C,D), the product ion at m/z 343.0523 was from the loss of one H₂O, and the fragment ion at m/z 199.0301 was obtained from the subsequent cracking of the C ring. Figure 6E summarizes the fragmentation pathways of PF 10 in the Q-TOF-MS/MS and LTQ-Orbitrap-MSⁿ ($n = 2–4$) results.

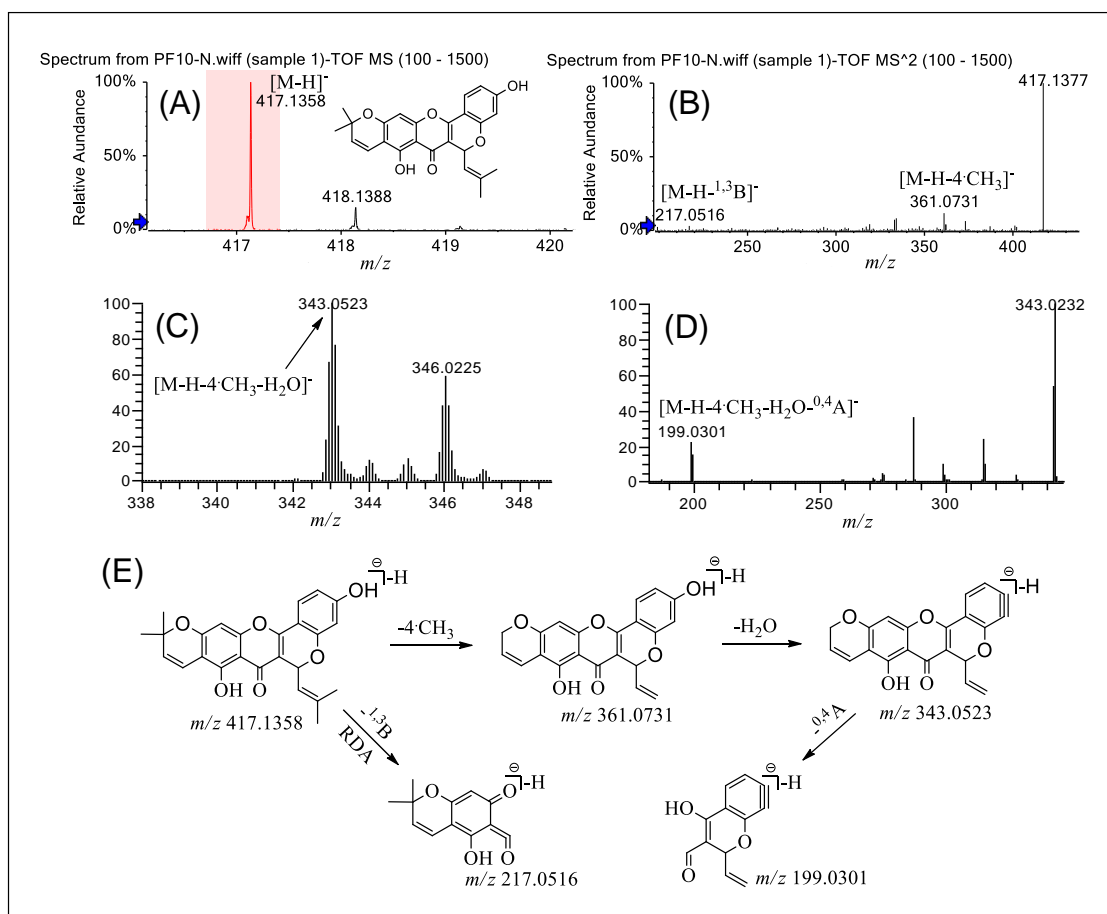


Figure 6. (–)ESI-Q-TOF-MS/MS and LTQ-Orbitrap-MSⁿ ($n = 3-4$) spectra of PF 10 in group B and the fragmentation pathways proposed for PF 10. Q-TOF-MS (A), Q-TOF-MS² (B), LTQ-Orbitrap-MS³ of the ions at m/z 361.0731 from m/z 417.1358 (C), LTQ-Orbitrap-MS⁴ of the ions at m/z 343.0523 from m/z 361.073 (D), and the proposed fragmentation pathways for PF 10 (E). RDA: retro Diels–Alder.

It is noteworthy that the compounds containing a free prenylated group at the C-8 position show some different fragmentation pathways. For the compound PF 11, the main fragmentation pathway is the loss of CO_2 from the C ring, generating the product ion at m/z 457.2002 ($[M - H - CO_2]^-$, error 3.94 ppm). However, for PF 10, the main pathway is the loss of H_2O . This difference can help us to determine the number and location of prenylated groups in compounds of this group.

2.6. Fragmentation of PFs 12–15

The four flavones in group E, with a dihydrobenzoxanthone skeleton, represent the characteristic constituents of the *Artocarpus* species, and this type of flavone has never been found in any other species. It was observed that dihydrobenzoxanthone-type flavone derivatives have a unique structure in which C–C linkage takes place between the C-6' position of the B ring and the C-12 position of the prenyl moiety located at the C-3 position. Because of this unique structure, the cleavage behavior of this type of flavonoid is different from that of other groups.

PF 12 was selected as an example to illustrate the fragmentation characteristics of this type of compound. Figure 7, Figures S65–S74 shows the typical ESI-MS spectra and cleavage pathways of PF 12 in negative ion mode for Q-TOF-MS/MS and LTQ-Orbitrap-MSⁿ ($n = 2-4$). The precursor ion $[M - H]^-$ of PF 12 at m/z 501.1943 (error 4.00 ppm) is shown in Figure 7A. The fragment ions at m/z 445.1296 ($[M - H - 4CH_3]^-$, error 0.47 ppm) and m/z 485.1626 ($[M - H - CH_4]^-$, error 4.12 ppm) correspond to the loss of $4CH_3$ or CH_4 from the molecular ion (Figure 7B). In the LTQ-Orbitrap-MS³⁻⁴ spectra (Figure 7C,D), we observed the initial loss of the H_2O group at the C-4' position from the fragment ion

(m/z 445.1296), and subsequently the loss of the CO group at the C-2' position, yielding prominent ions at m/z 399.1040 $[M - H - 4\text{-CH}_3 - \text{H}_2\text{O} - \text{CO}]^-$. In addition, Figure 7E,F illustrates the successive losses of CO and another four $\cdot\text{CH}_3$ in the fragmentation $[M - H - \text{CH}_4]^-$, producing the product ions $[M - H - \text{CH}_4 - \text{CO}]^-$ (m/z 457.1961), $[M - H - \text{CH}_4 - 4\text{-CH}_3]^-$ (m/z 429.1201), and $[M - H - \text{CH}_4 - 4\text{CH}_3 - \text{CO}]^-$ (m/z 401.1094). The three other compounds in this group also showed the same fragmentation patterns as PF 12. Thus, Figure 7G summarizes the possible fragmentation pathway of PF 12. This fragmentation pathway makes it easier to determine the structural characteristics of these compounds.

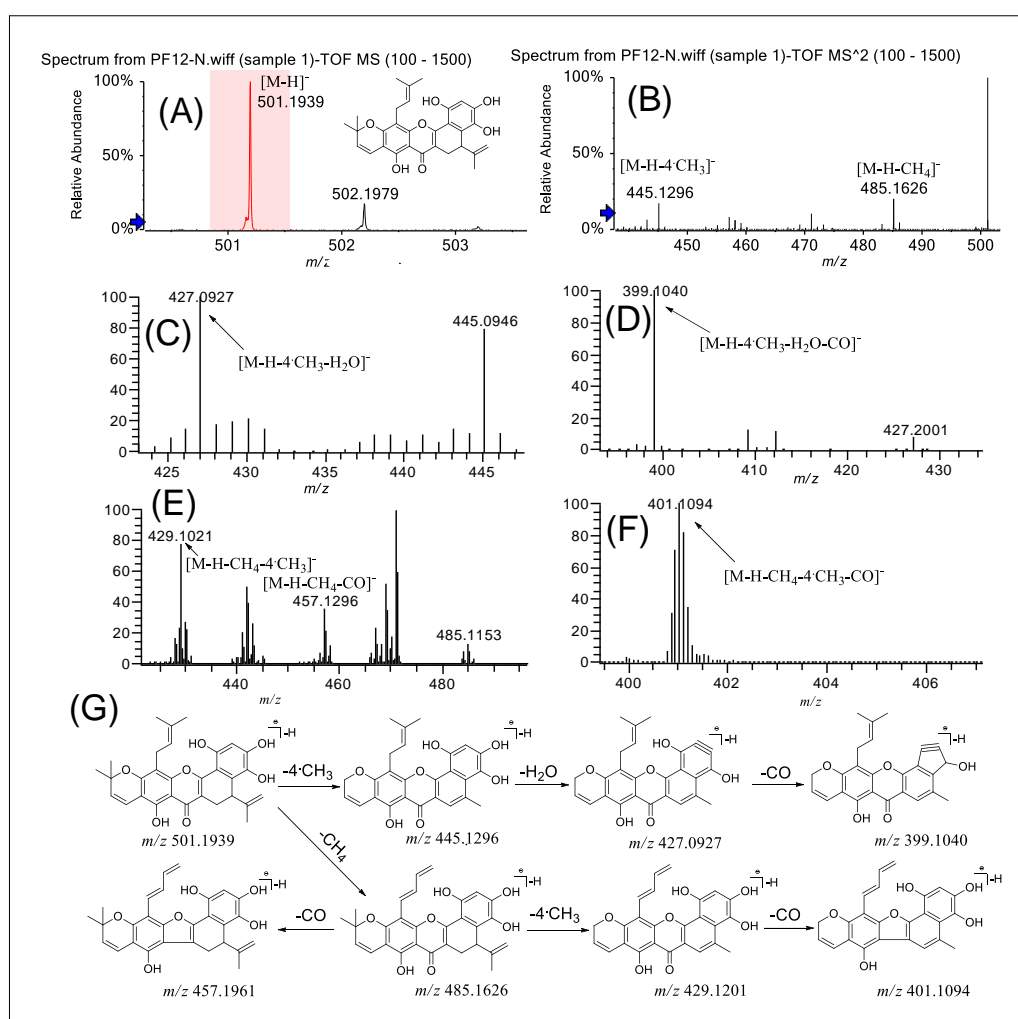


Figure 7. (–)ESI-Q-TOF-MS/MS and LTQ-Orbitrap-MSⁿ ($n = 3-4$) spectra of PF 12 in group B and the fragmentation pathways proposed for PF 12. Q-TOF-MS (A), Q-TOF-MS² (B), LTQ-Orbitrap-MS³ of the ions at m/z 445.1296 from m/z 501.1939 (C), LTQ-Orbitrap-MS⁴ of the ions at m/z 427.0927 from at m/z 445.1296 (D), LTQ-Orbitrap-MS³ of the ions at m/z 485.1631 from m/z 501.1939 (E), LTQ-Orbitrap-MS⁴ of the ions at m/z 429.1201 from m/z 485.1631 (F), and the proposed fragmentation pathways for PF 12 (G).

2.7. Rapid Identification of PFs in the Extract of *A. heterophyllum* Roots

The PFs in the extract of *A. heterophyllum* roots were analyzed by UPLC-Q-TOF-MS/MS, and the total ion chromatogram (TIC) of the sample in negative ion mode was obtained, as shown in Figure 8A. Based on the existing literature and our previous studies, a total of 47 PFs were identified in the extract of *A. heterophyllum* roots. The formulae of the 47 compounds were accurately assigned within a relative theoretical mass error of 5 ppm, and the relative theoretical mass errors of the characteristic fragment ions were all within 10 ppm. The identification process of the detected compounds was as follows [22]. Firstly, an accurate molecular mass was obtained via the high-resolution Q-TOF-MS

technique according to the deprotonated ion $[M - H]^-$. Secondly, the formula was obtained by Peakview software according to the accurate molecular mass, constituent elements, and isotope abundance. Thirdly, the differentiation and characterization of the analytes were completed by considering the product ions, fragmentation pathways, and literature data. The related information is summarized in Table 2, including the compound name, molecular formula, precursor ion, characteristic fragment ions, and the error. The identified compounds were validated by extracting the relative characteristic fragmentations, such as precursor ions, nuclear parent ions, and daughter ions (Figure 8). The following examples are given to illustrate the identification process of the PFs.

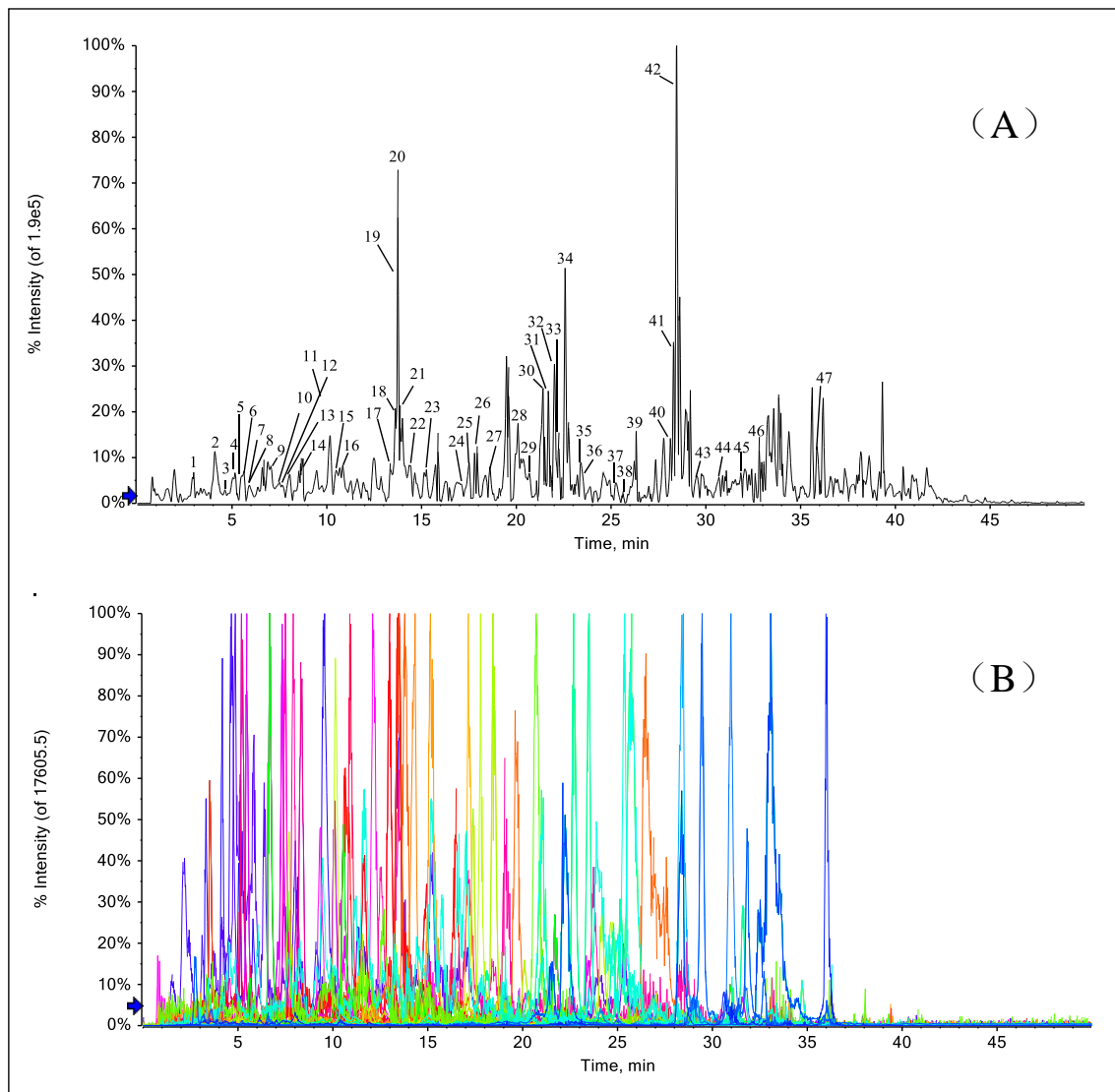


Figure 8. Total ion chromatogram (A) and extracted ion chromatogram (B) of prenylated flavonoids in the extract of *Artocarpus heterophyllus* Lam. roots.

Table 2. The 47 prenylated flavonoids identified from the extract of *Artocarpus heterophyllus* Lam. roots.

Peak No.	Compounds	RT (min)	Molecular Formula	[M – H] [–] (m/z)	Error (Δppm)	Product Ions (m/z)	Error (Δppm)	Fragment Ions Identified
1	6-(3-Methylbutyl-2-enyl)apigenin [23]	3.49	C ₂₀ H ₁₈ O ₅	337.10903	2.6	219.0681	8.2	[M – H – ^{1,3} B] [–]
2	Artonin K [24]	4.14	C ₂₁ H ₁₈ O ₇	381.09924	3.3	281.0473	6.4	[M – H – C ₄ H ₈] [–]
3	Albanin A [25]	4.66	C ₂₀ H ₁₈ O ₆	353.10459	4.3	337.0738	5.9	[M – H – C ₂ H ₄ O] [–]
4	14-Hydroxyartoinin E [26]	4.87	C ₂₅ H ₂₄ O ₈	451.14188	4.5	365.0687	5.5	[M – H – CH ₄] [–]
5	Artoindonesianin P [27]	5.22	C ₂₂ H ₂₀ O ₇	395.11548	4.7	125.0246	4.8	[M – H – ^{1,4} B] [–]
6	Artonin J [28]	5.47	C ₂₅ H ₂₄ O ₇	435.14663	3.9	231.0668	2.2	[M – H – ^{1,4} A] [–]
7	Artelastoxanthone [18]	6.67	C ₂₅ H ₂₂ O ₇	433.12925	–0.1	393.0999	4.8	[M – H – C ₃ H ₆ O] [–]
8	Artobiloxanthone [29]	6.68	C ₂₅ H ₂₂ O ₇	433.13224	6.8	433.1289	0.9	[M – H – H ₂ O] [–]
9	Artonin E [28]	7.23	C ₂₅ H ₂₄ O ₇	435.14663	3.9	337.0736	5.3	[M – H – C ₃ H ₆ O] [–]
10	Cyclocommunol [30]	7.31	C ₂₀ H ₁₆ O ₆	351.08818	2.2	351.0515	1.4	[M – H – 3·CH ₃] [–]
11	Artoindonesianin Q [4]	7.47	C ₂₂ H ₂₂ O ₇	397.12891	–0.9	379.0839	4.2	[M – H – C ₄ H ₈] [–]
12	Artoindonesianin R [31]	7.49	C ₂₂ H ₂₂ O ₇	397.13136	5.1	365.0681	3.8	[M – H – C ₅ H ₁₀] [–]
13	Artonol E [32]	7.91	C ₂₆ H ₂₄ O ₇	447.14548	1.2	405.1399	–1.2	[M – H – CO] [–]
14	Artoindonesianin T [31]	8.31	C ₂₂ H ₂₀ O ₇	395.11548	4.7	389.1017	3.6	[M – H – CO ₂] [–]
15	Cycloartobiloxanthone [27]	10.48	C ₂₅ H ₂₂ O ₇	433.13134	4.7	405.1364	4.9	[M – H – CO] [–]
						403.0850	6.7	[M – H – 2CH ₃] [–]
						379.0841	4.7	[M – H – C ₄ H ₈] [–]
						351.0887	3.7	[M – H – C ₅ H ₄ O] [–]
						199.0777	6.0	[M – H – ^{1,3} A] [–]
						295.0259	3.7	[M – H – C ₄ H ₈] [–]
						137.0247	–2.2	[M – H – ^{1,4} B] [–]
						313.0345	2.9	[M – H – CH ₃ – C ₅ H ₉] [–]
						311.0195	0.6	[M – H – OCH ₃ – C ₄ H ₇] [–]
						365.1021	–2.2	[M – H – OCH ₃] [–]
						313.0357	1.0	[M – H – C ₆ H ₁₂] [–]
						137.0242	–1.5	[M – H – ^{1,4} B] [–]
						415.1155	–7.7	[M – H – OCH ₄] [–]
						391.0831	2.0	[M – H – C ₄ H ₈] [–]
						339.0518	2.4	[M – H – C ₄ H ₈] [–]
						365.0655	–3.3	[M – H – 2CH ₃] [–]
						391.0824	0.3	[M – H – C ₃ H ₆] [–]
						415.1177	–2.4	[M – H – H ₂ O] [–]

Table 2. Cont.

Peak No.	Compounds	RT (min)	Molecular Formula	[M – H] [–] (m/z)	Error (Δppm)	Product Ions (m/z)	Error (Δppm)	Fragment Ions Identified
16	Artoindonesianin B [33]	10.92	C ₂₆ H ₂₈ O ₈	467.17322	4.4	261.0758	–3.8	[M – H – ^{1,4} A] [–]
17	Artocarpetin A [34]	13.07	C ₂₁ H ₂₀ O ₆	367.11769	–2.8	451.1399	0.2	[M – H – CH ₄] [–]
						233.0829	–4.3	[M – H – ^{1,3} B] [–]
						297.0410	–1.7	[M – H – C ₅ H ₁₀] [–]
18	Heteroflavanone C [35]	13.44	C ₂₃ H ₂₆ O ₇	413.16078	0.5	309.0763	1.6	[M – H – C ₃ H ₄ O] [–]
						247.0975	–0.4	[M – H – C ₉ H ₁₀ O ₃] [–]
						235.0982	2.6	[M – H – ^{1,2} B] [–]
19	Artocarpesin [36]	13.48	C ₂₀ H ₁₈ O ₅	337.10903	2.6	133.0294	–0.8	[M – H – ^{1,3} A] [–]
20	6-(3-Methylbut-2-enyl) Apigenin [18]	13.5	C ₂₀ H ₁₈ O ₅	337.10809	–0.2	281.0477	7.8	[M – H – C ₄ H ₈] [–]
						281.0464	–3.2	[M – H – C ₄ H ₈] [–]
21	Styracifolin D [4]	13.88	C ₃₀ H ₃₂ O ₈	519.20258	0.3	117.0349	–2.6	[M – H – ^{1,3} A] [–]
						461.1583	5.0	[M – H – C ₃ H ₆ O] [–]
						491.2075	0.0	[M – H – CO] [–]
22	Cycloartocarpesin [37]	14.28	C ₂₀ H ₁₆ O ₅	335.09274	0.7	501.1919	0.0	[M – H – H ₂ O] [–]
						133.0301	4.5	[M – H – ^{1,3} A] [–]
						305.0462	2.3	[M – H – 2CH ₃] [–]
23	Artonin U [38]	15.17	C ₂₁ H ₂₀ O ₅	351.12462	2.4	281.0469	5.0	[M – H – C ₅ H ₁₀] [–]
24	Norartocarpin [39]	17.16	C ₂₅ H ₂₆ O ₆	421.16567	0	227.0725	4.8	[M – H – ^{1,4} A] [–]
						309.0391	–4.5	[M – H – C ₈ H ₁₆] [–]
						365.1009	–6.0	[M – H – C ₄ H ₈] [–]
25	Mulberrochromene [40]	17.50	C ₂₅ H ₂₄ O ₆	419.15040	0.9	199.0781	8.0	[M – H – ^{1,3} A] [–]
						349.0726	2.3	[M – H – C ₅ H ₁₀] [–]
						191.0715	0.5	[M – H – ^{1,4} B] [–]
26	Dihydroisocycloartomunin [31]	17.79	C ₂₆ H ₂₆ O ₇	449.16080	0.5	365.0694	7.4	[M – H – C ₆ H ₁₂] [–]
						191.0728	7.3	[M – H – ^{1,4} B] [–]
27	Morusin [41]	18.48	C ₂₅ H ₂₄ O ₆	419.15040	0.9	217.0515	4.1	[M – H – ^{1,3} B] [–]
						227.0725	4.8	[M – H – ^{1,4} A] [–]
						217.0515	4.1	[M – H – ^{1,4} B] [–]
28	Heterophyllin [17]	20.55	C ₃₀ H ₃₂ O ₇	503.20842	2.1	217.0879	4.1	[M – H – ^{1,3} A] [–]
						243.0662	–0.4	[M – H – ^{1,4} A] [–]
						259.1351	4.2	[M – H – ^{1,4} B] [–]
						285.1112	5.6	[M – H – ^{1,3} B] [–]

Table 2. Cont.

Peak No.	Compounds	RT (min)	Molecular Formula	[M – H] [–] (m/z)	Error (Δppm)	Product Ions (m/z)	Error (Δppm)	Fragment Ions Identified
29	Artocarpetin B [42]	20.72	C ₂₂ H ₂₂ O ₆	381.13518	2.2	233.0806	–5.6	[M – H – ^{1,3} B] [–]
30	Artelastofuran [43]	21.07	C ₃₀ H ₃₄ O ₇	505.22363	0.9	311.0549	–3.9	[M – H – C ₅ H ₁₀] [–]
31	5'-Hydroxycudraflavone A [17]	21.81	C ₂₅ H ₂₂ O ₇	433.12925	–0.1	277.1455	3.6	[M – H – ^{1,4} B] [–]
32	Artonin F [44]	22.04	C ₃₀ H ₃₀ O ₇	501.19231	0.9	285.1147	5.3	[M – H – ^{0,3} B] [–]
33	Isocycloheterophyllin [45]	22.23	C ₃₀ H ₃₀ O ₇	501.19290	–2.0	389.1372	5.7	[M – H – CO ₂] [–]
34	Artoindonesianin I [46]	22.70	C ₃₀ H ₃₄ O ₇	505.22363	0.9	415.1192	–1.2	[M – H – H ₂ O] [–]
35	Artocarpin [47]	23.48	C ₂₆ H ₂₈ O ₆	435.18167	0.8	217.0516	–4.6	[M – H – ^{1,3} A] [–]
36	Cannflavin C [20]	23.59	C ₂₆ H ₂₈ O ₆	435.18022	–2.5	377.0663	1.1	[M – H – C ₃ H ₄ O] [–]
37	Artonin H [44]	25.10	C ₃₀ H ₃₄ O ₇	505.22363	0.9	429.1343	–0.2	[M – H – C ₄ H ₈ O] [–]
38	Artonin S [38]	25.36	C ₂₆ H ₂₈ O ₇	451.17621	0.0	473.1945	–5.3	[M – H – CO] [–]
39	Artonin G [44]	26.21	C ₃₀ H ₃₂ O ₇	503.20862	2.2	445.1267	–2.2	[M – H – CH ₄] [–]
40	Artonin A [48]	28.15	C ₃₀ H ₃₀ O ₇	501.19231	0.9	485.1615	–1.9	[M – H – C ₃ H ₄ O] [–]
41	Artonin B [48]	28.39	C ₃₀ H ₃₀ O ₇	501.19230	0.8	443.1511	–2.5	[M – H – C ₃ H ₆ O] [–]
42	Cudraflavone A [49]	28.41	C ₂₅ H ₂₂ O ₆	417.13475	0.9	285.1137	1.8	[M – H – ^{0,3} B] [–]
						447.1806	–1.6	[M – H – C ₃ H ₆ O] [–]
						207.1039	5.8	[M – H – ^{1,4} B] [–]
						233.0818	–0.4	[M – H – ^{1,3} B] [–]
						351.0878	–1.1	[M – H – C ₆ H ₁₂] [–]
						323.0939	–4.3	[M – H – C ₆ H ₇ – OCH ₃] [–]
						313.1452	–2.2	[M – H – C ₉ H ₁₄] [–]
						191.0728	7.3	[M – H – ^{1,4} B] [–]
						217.0512	2.8	[M – H – ^{1,3} B] [–]
						393.1357	3.3	[M – H – C ₃ H ₆ O] [–]
						421.1311	4.3	[M – H – 2CH ₃] [–]
						447.1422	–6.0	[M – H – C ₄ H ₈] [–]
						475.2103	–4.8	[M – H – CO] [–]
						457.1286	–1.5	[M – H – C ₃ H ₈] [–]
						473.1950	–4.2	[M – H – CO] [–]
						485.1602	0.8	[M – H – CH ₄] [–]
						445.1296	–0.7	[M – H – C ₃ H ₄ O] [–]
						217.0515	4.1	[M – H – ^{1,3} B] [–]
						373.1072	–2.4	[M – H – C ₂ H ₄ O] [–]

Table 2. Cont.

Peak No.	Compounds	RT (min)	Molecular Formula	[M – H] [–] (m/z)	Error (Δppm)	Product Ions (m/z)	Error (Δppm)	Fragment Ions Identified
43	Artoindonesianin G [46]	29.45	C ₃₀ H ₃₂ O ₆	487.21308	1.0	259.1351 285.1116 365.1762	4.2 –5.6 1.1	[M – H – ^{1,4} B] [–] [M – H – ^{1,3} B] [–] [M – H – C ₇ H ₆ O ₂] [–]
44	Cycloartocarpin [50]	30.97	C ₂₆ H ₂₆ O ₆	433.16608	1.0	199.0777 363.0878 375.0878	6.0 1.1 1.1	[M – H – ^{1,3} A] [–] [M – H – C ₅ H ₁₀] [–] [M – H – C ₄ H ₁₀] [–]
45	Artoindonesianin H [46]	31.80	C ₃₀ H ₃₂ O ₆	487.21308	1.0	227.0731 361.0731 473.1966	7.5 3.6 –0.8	[M – H – C ₉ H ₁₈] [–] [M – H – ^{1,4} A] [–] [M – H – CO] [–]
46	Cycloheterophyllin [17]	33.05	C ₃₀ H ₃₀ O ₇	501.19231	0.9	285.1145 445.1281 473.1966	4.6 –2.7 –0.8	[M – H – ^{1,3} B] [–] [M – H – C ₄ H ₈] [–] [M – H – CO] [–]
47	Artelastochromene [43]	36.01	C ₃₀ H ₃₀ O ₆	485.19690	–0.1	285.1145 469.1659	4.6 0.4	[M – H – ^{1,3} B] [–] [M – H – CH ₄] [–]

The precursor ion and fragment ions of peaks 3, 7, 17, 33 and 41 in the TIC profile of *A. heterophyllum* root extract are basically the same as those for PFs 6, 13, 1, 15 and 12 discussed in this experiment. Therefore, compounds 3, 7, 17, 33 and 41 were identified as PFs 6, 13, 1, 15 and 12. The precursor ions of compounds 11 and 28 were m/z 397.1289 ($[M - H]^-$) and m/z 503.2068 ($[M - H]^-$), respectively, affording the molecular formulae $C_{22}H_{22}O_7$ and $C_{30}H_{32}O_7$ with errors of -0.9 and -1.4 ppm, respectively. In the Q-TOF-MS/MS spectra, these two compounds have $^{1,4}A^-$, $^{1,4}B^-$ fragments. According to the fragmentation pattern of group C, it can be inferred that both of them have a prenylated substitution in the C-3 position. In addition, the fragment ions of compound 10 included $[M - H - 2OCH_3]^-$ (m/z 335.0935). It can be inferred that compound 11 may contain two OCH_3 . By comparison with our data [4], compound 11 was identified as artoindonesianin Q. Compound 28 also produced a low abundance of RDA fragments. Based on the fragmentation pattern of group C, the C-8 position of compound 28 may contain a prenylated group, but there is no ortho effect. It is possible that there is no free phenolic hydroxyl at the C-7 position. Based on the related literature [17] and retention time, compound 28 was identified as heterophyllin.

Compound 31 produced a 433.1293 $[M - H]^-$ precursor ion in negative ion mode. It was inferred that its molecular formula is $C_{25}H_{22}O_7$, and the error was -0.1 ppm. The characteristic fragment ions of compound 31 include $[M - H - CO_2]^-$ (m/z 389.1372), $[M - H - H_2O]^-$ (m/z 415.1192), and $[M - H - ^{1,3}A]^-$ (m/z 217.0516). It can be inferred that in compound 30, there is a 3-prenyl side chain forming a pyran ring with HO-6' of the B ring, and C-3' and C-4' of the B ring contain two free phenolic hydroxyl groups. This is basically consistent with the fragmentation pathway of group D. This information suggested that this compound should be 5'-hydroxycudraflavone [17]. The precursor ion of compound 39 ($[M - H]^-$ ion at m/z 503.2086) afforded the molecular formula $C_{30}H_{32}O_7$ with an error of 2.2 ppm. The fragmentations $[M - H - C_4H_8]^-$ at m/z 447.1422 and $[M - H - CO]^-$ at m/z 475.2103 indicated that this compound was artonin G [44]. This is basically consistent with the fragmentation pathway of group E.

3. Materials and Methods

3.1. Plant Material

The roots of *A. heterophyllum* were collected from Nanning city, Guangxi Zhuang Autonomous Region, China, in April 2017 and authenticated by Associate Researcher Lv Shihong of Guangxi Institute of Botany, Chinese Academy of Sciences. The voucher specimen (TCM20170502) was deposited in the Herbarium of the Department of Pharmacognosy, Research Center of Natural Resources of Chinese Medicinal Materials and Ethnic Medicine, Jiangxi University of Traditional Chinese Medicine, Nanchang, China.

3.2. Model Molecules and Reagents

A total of 15 PFs (PFs 1–15) were isolated from *Artocarpus* plants in our previous studies [17–20]. Their structures (Figure 1) were unequivocally elucidated by spectroscopic methods, including one-dimensional and two-dimensional nuclear magnetic resonance, high-resolution electrospray ionization mass spectroscopy, and infrared spectroscopy. The purity of these compounds was determined to be higher than 98% by normalizing the peak area using high-performance liquid chromatography (HPLC) equipped with a diode array detector (DAD). Chromatographic-grade acetonitrile (ACN) and methanol were purchased from Tedia Co. Inc. Deionized water was prepared using a Milli-Q water purification system (Millipore, USA).

3.3. Sample Preparation

The air-dried and powdered roots of *A. heterophyllum* (50.0 g) were extracted with 95% EtOH three times (500 mL for each extraction) at room temperature. The filtrate was evaporated in vacuo to produce a residue (4.2 g) which was loaded on an HP-20 macroporous resin column chromatograph

and eluted successively with a gradient of EtOH/H₂O (0:100 and 95:5, *v/v*) to give two fractions. The 95% EtOH elution fraction was concentrated to afford a residue. The dried residue was re-dissolved in 50 mL of methanol in a volumetric flask; then, the samples were filtered through a 0.22 µm membrane prior to analysis.

3.4. Ultra-High Performance Liquid Chromatography (UPLC)-Q-TOF-MS/MS and UPLC-LTQ-Orbitrap-MSⁿ Analysis of PFs

A TripleTOF AB 5600⁺ high-resolution mass spectrometer (AB SCIEX, Framingham, USA) was used to obtain primary and secondary mass spectrometry data by the UPLC-Q-TOF-MS/MS method. The AB mass spectrometer was equipped with an electrospray ionization (ESI) ion source and an LC-30A ultra-high-performance liquid chromatograph (Shimadzu, Japan). The multistage mass spectrometry data were obtained using a Thermo Fisher LTQ-Orbitrap Electrostatic Mass Spectrometer (Thermo Fisher Scientific, Bremen, Germany).

In the UPLC-Q-TOF/MS analysis, the chromatographic separation was carried out on an ACQUIT UPLC[®] BEH (1.7 µm, 2.1 × 50 mm, Water, Milford, MA, USA). The mobile phase was composed of 30% ultrapure water and 70% methanol with a flow rate of 0.3 mL/min, and the injection volume was 2.0 µL. The mobile phase for the extracts was ultrapure water (A) and methanol (B) using a gradient elution program: 45–60% B at 0–2 min, 60–65% B at 2–10 min, 65–70% B at 10–25 min, 70–80% B at 25–30 min, 80–100% B at 30–40 min, then held for 10 min. Q-TOF-MS analysis was performed in negative ion mode using full scan mode with a mass range of 100–1500 Da. The MS parameters were optimized as follows: ion spray voltage, −4500 V; source temperature, 550 °C; curtain gas, 30 psi; nebulizer gas (GS1), 50 psi; heater gas (GS2), 50 psi; de-clustering potential (DP), −100 V; and pre-scan and trigger second-stage scan time of Q-TOF-MS, 250 and 100 ms, respectively. AB Analyst TF Software (AB SCIEX, Framingham, USA) was used to collect data. The collision energy (CE) and collision energy superposition (CES) of each compound were optimized.

The Thermo Fisher LTQ-Orbitrap Electrostatic Mass Spectrometer was used in ESI negative ion mode and multistage scanning mode. The optimized parameters were as follows: capillary temperature, 320 °C; ion source heater, 300 °C; source voltage, 3.6 kV; sheath gas (N₂), 35 arbitrary units; aux gas, 10 arbitrary units; sweep gas flow, 0 arbitrary units; S-Lens RF level (%): 60%; CE, 30 eV; and CES, 10 eV. The experiments were performed in negative mode, scanning from *m/z* 100 to 1000.

3.5. Data Preprocessing Analysis

The data collected via UHPLC-Q-TOF-MS/MS were processed using Peak View 1.2 software (AB SCIEX, version 1.2.0.3) from AB Sciex Company. The empirical molecular formulae were deduced from Peakview by comparing the theoretical masses of molecular ions and/or adductions with the determined values based on the following error limits: mass accuracy, < 5 ppm; retention time, < 5.0%; and isotope abundance, < 10%. The multistage mass spectrometry data collected via ESI-LTQ-Orbitrap-MSⁿ were processed using Thermo Xcalibur 2.2 (Thermo Fisher Scientific).

4. Conclusions

In this work, 15 PFs from *Artocarpus* plants served as standards and were divided into five types according to their structural characteristics with respect to the position and existence of prenyl substitution in the flavone skeleton. A data acquisition strategy based on the combination of Q-TOF-MS and LTQ-Orbitrap-MSⁿ was used to obtain both [M − H][−] and product ion information. Fragmentation rules for the five groups were summarized, and possible fragmentation pathways were proposed. These fragmentation rules were successfully exploited to qualitatively analyze the PFs from *A. heterophyllus*, a well-known *Artocarpus* plant; a total of 47 PFs were identified from the extract of this plant. These results indicate that the developed analytical method could be used as a rapid, effective technique for the qualitative characterization of PFs in *Artocarpus* plants and in other PF-accumulating medicinal herbs.

Supplementary Materials: The following are available online, Figures S1–S5: (–)ESI-Q-TOF-MS/MS and -LTQ-Orbitrap-MSⁿ spectra of PF 1; Figures S6–S11: (–)ESI-Q-TOF-MS/MS and -LTQ-Orbitrap-MSⁿ spectra of PF 2; Figures S12–S15: (–) ESI-Q-TOF-MS/MS and -LTQ-Orbitrap-MSⁿ spectra of PF 3; Figures S16–S19: (–) ESI-Q-TOF-MS/MS and -LTQ-Orbitrap-MSⁿ spectra of PF 4; Figures S20–S24: (–) ESI-Q-TOF-MS/MS and -LTQ-Orbitrap-MSⁿ spectra of PF 5; Figures S25–S29: (–) ESI-Q-TOF-MS/MS and -LTQ-Orbitrap-MSⁿ spectra of PF 6; Figures S30–S35: (–) ESI-Q-TOF-MS/MS and -LTQ-Orbitrap-MSⁿ spectra of PF 7; Figures S36–S41: (–) ESI-Q-TOF-MS/MS and -LTQ-Orbitrap-MSⁿ spectra of PF 8; Figures S42–S46: (–) ESI-Q-TOF-MS/MS and -LTQ-Orbitrap-MSⁿ spectra of PF 9; Figures S47–S50: (–) ESI-Q-TOF-MS/MS and -LTQ-Orbitrap-MSⁿ spectra of PF 10; Figures S51–S56: (–) ESI-Q-TOF-MS/MS and -LTQ-Orbitrap-MSⁿ spectra of PF 11; Figures S57–64: (–) ESI-Q-TOF-MS/MS and -LTQ-Orbitrap-MSⁿ spectra of PF 12; Figures S65–S74: (–) ESI-Q-TOF-MS/MS and -LTQ-Orbitrap-MSⁿ spectra of PF 13; Figures S75–S81: (–) ESI-Q-TOF-MS/MS and -LTQ-Orbitrap-MSⁿ spectra of PF 14; Figures S82–S89: (–) ESI-Q-TOF-MS/MS and -LTQ-Orbitrap-MSⁿ spectra of PF 15.

Author Contributions: Conceptualization, G.R., and J.-B.Y. (Jin-Bao Ye); Formal analysis, J.-B.Y. (Jin-Bao Ye); Methodology, J.-B.Y. (Jin-Bao Ye), G.R., W.-Y.L., and T.L.; Resources, G.-Y.Z. and M.Z.; Writing—original draft, G.R. and J.-B.Y. (Jin-Bin Yuan); Writing—review and editing, J.-B.Y. (Jin-Bao Ye) and J.-B.Y. (Jin-Bin Yuan). All authors reviewed and approved the final manuscript.

Funding: This work was financially supported by the National Natural Science Foundation of China (Grant No. 81160509, 81360475), the Young Scientist Development Program of Jiangxi Province (Grant No. 20142BCB23024), the Jiangxi provincial natural science fund project (Grant No. 20151BAB205074), the Double First-class Discipline of Jiangxi Province (Grant No. JXSYLXK-ZHYAO027, JXSYLXK-ZHYAO064), and the Graduate student innovation special fund project of Jiangxi University of Traditional Chinese Medicine (Grant No. JZYC19S47).

Conflicts of Interest: The authors declare no conflict of interest.

References

1. Liou, S.S.; Shieh, W.L.; Chen, T.H.; Won, S.J.; Lin, C.N. γ -Pyrone compounds as potential anti-cancer drugs. *J. Pharm. Pharmacol.* **1993**, *45*, 791–794. [[CrossRef](#)] [[PubMed](#)]
2. Hu, X.; Wu, J.W.; Wang, M.; Yu, M.H.; Zhao, Q.S.; Wang, H.Y.; Hou, A.J. 2-Arylbzofuran, flavonoid, and tyrosinase inhibitory constituents of *Morus yunnanensis*. *J. Nat. Prod.* **2012**, *75*, 82–87. [[CrossRef](#)] [[PubMed](#)]
3. Patil, A.D.; Freyer, A.J.; Killmer, L.; Offen, P.; Taylor, P.B.; Votta, B.J.; Johnson, R.K. A new dimeric dihydrochalcone and a new prenylated flavone from the bud covers of *Artocarpus altilis*: Potent inhibitors of cathepsin k. *J. Nat. Prod.* **2002**, *65*, 624–627. [[CrossRef](#)] [[PubMed](#)]
4. Yuan, W.J.; Yuan, J.B.; Peng, J.B.; Ding, Y.Q.; Zhu, J.X.; Ren, G. Flavonoids from the roots of *Artocarpus heterophyllus*. *Fitoterapia* **2017**, *117*, 133–137. [[CrossRef](#)]
5. Bourjot, M.; Apel, C.; Martin, M.T.; Grellier, P.; Nguyen, V.H.; Gueritte, F.; Litaudon, M. Antiplasmodial, antitypanosomal, and cytotoxic activities of prenylated flavonoids isolated from the stem bark of *Artocarpus styracifolius*. *Planta Med.* **2010**, *76*, 1600–1604. [[CrossRef](#)]
6. Hanáková, Z.; Hošek, J.; Kutil, Z.; Temml, V.; Landa, P.; Vaněk, T.; Schuster, D.; Dall'Acqua, S.; Cvačka, J.; Polanský, O.; et al. Anti-inflammatory activity of natural geranylated flavonoids: Cyclooxygenase and lipoxygenase inhibitory properties and proteomic analysis. *J. Nat. Prod.* **2017**, *80*, 999–1006. [[CrossRef](#)]
7. Ren, G.; Xiang, H.Y.; Hu, Z.C.; Liu, R.H.; Yi, W.F.; Peng, J.B.; Yuan, J.B. Inhibitory effects of phenolic compounds from *Artocarpus styracifolius* on respiratory burst of rat neutrophils. *Pharm. Biol.* **2014**, *52*, 944–950. [[CrossRef](#)]
8. Nomura, T.; Hano, Y.; Aida, M. Isoprenoid-substituted flavonoids from *Artocarpus* plants (Moraceae). *Heterocycles* **1998**, *47*, 1179–1205. [[CrossRef](#)]
9. Ren, G.; Peng, J.B.; Yi, W.F.; Yuan, W.J. Advance on chemical constituents from *Artocarpus* plant and its bioactivities in recent five years. *Chin. J. Exp. Tradit. Med. Formul.* **2014**, *20*, 234–239.
10. Zhang, X.S.; Wu, Z.Y. *Zhongguo Zhiwu Zhi (Flora of China)*; Science Press: Beijing, China, 1998.
11. Li, Y.; Mao, Q.; Feng, F.; Ye, C. Genetic diversity within a jackfruit (*Artocarpus heterophyllus* Lam.) germplasm collection in China using AFLP markers. *Agric. Sci. China* **2010**, *9*, 1263–1270. [[CrossRef](#)]
12. Nguyen, N.T.; Nguyen, M.H.; Nguyen, H.X.; Bui, N.K.; Nguyen, M.T. Tyrosinase inhibitors from the wood of *Artocarpus heterophyllus*. *J. Nat. Prod.* **2012**, *75*, 1951–1955. [[CrossRef](#)] [[PubMed](#)]
13. Zheng, Z.P.; Xu, Y.; Qin, C.; Zhang, S.; Gu, X.; Lin, Y.; Xie, G.; Wang, M.; Chen, J. Characterization of antiproliferative activity constituents from *Artocarpus heterophyllus*. *J. Agric. Food Chem.* **2014**, *62*, 5519–5527. [[CrossRef](#)] [[PubMed](#)]

14. Sun, X.Y.; Zhang, Y.B.; Chen, S.Q.; Fu, Y. Characterization and identification of the chemical constituents in the root of *Lindera reflexa* Hemsl. using ultra-high performance liquid chromatography coupled with linear trap quadrupole orbitrap mass spectrometry. *J. Pharm. Biomed. Anal.* **2016**, *126*, 34–47. [[CrossRef](#)] [[PubMed](#)]
15. Lin, S.; Ye, J.; Liang, X.; Zhang, X.; SU, J.; Fu, P.; Lv, D.Y.; Zhang, W.D. Mass spectrometric profiling of valepotriates possessing various acyloxy groups from *Valeriana jatamansi*. *J. Mass Spectrom.* **2015**, *50*, 1294–1304. [[CrossRef](#)]
16. Kang, L.P.; Zhao, Y.; Pang, X.; Yu, H.S.; Xiong, C.Q.; Zhang, J.; Gao, Y. Characterization and identification of steroidal saponins from the seeds of *Trigonella foenum-graecum* by ultra high-performance liquid chromatography and hybrid time-of-flight mass spectrometry. *J. Pharm. Biomed. Anal.* **2013**, *74*, 257–267. [[CrossRef](#)]
17. Zhai, X.X.; Zhong, G.Y.; Yao, P.C.; Lin, Q.H.; Yuan, W.J.; Ren, G. Phenolic constituents from root of *Arocarpus heterophyllus*. *Chin. Tradit. Herb. Drugs* **2016**, *47*, 3959–3964.
18. Xiao, C.Y.; Li, W.Y.; Zhai, X.X.; Zhu, L.Z.; Zhou, Y.F.; Yao, P.C.; Shu, Q.X.; Ren, G. Prenylated flavonoids from the roots of *Artocarpus heterophyllus*. *Acta Pharm. Sin.* **2018**, *53*, 592–597.
19. Lin, Q.H.; Yuan, J.B.; Ma, Z.L.; Liang, J.; Zhai, X.X.; Khan, I.A.; Ding, Y.Q.; Ren, G. Isoprenylated flavonoids from roots of *Artocarpus styracifolius*. *Nat. Prod. Commun.* **2016**, *11*, 1843–1846.
20. Lin, Q.H.; Yao, P.C.; Xiao, C.Y.; Zhai, X.X.; Yuan, W.J.; Ren, G. Chemical constituents from the root of *Artocarpus stracifolius*. *J. Chin. Med. Mater.* **2017**, *40*, 839–844.
21. Simons, R.; Vincken, J.P.; Bohin, M.C.; Kuijpers, T.F.M.; Verbruggen, M.A.; Gruppen, H. Identification of prenylated pterocarpan and other isoflavonoids in *Rhizopus spp.* elicited soya bean seedlings by electrospray ionisation mass spectrometry. *Rapid Commun. Mass Spectrom.* **2010**, *25*, 55–65. [[CrossRef](#)]
22. Yu, L.; Wei, F.; Liang, J.; Ren, G.; Liu, X.; Wang, C.Z.; Yuan, J.; Zeng, J.; Luo, Y.; Bi, Y.; et al. Target molecular-based neuroactivity screening and analysis of *Panax ginseng* by affinity ultrafiltration, UPLC-QTOF-MS and molecular docking. *Am. J. Chin. Med.* **2019**, *47*, 1345–1363. [[CrossRef](#)] [[PubMed](#)]
23. Abegaz, B.M.; Ngadjui, B.T.; Dongo, E.; Tamboue, H. Prenylated chalcones and flavones from the leaves of *Dorstenia kameruniana*. *Phytochemistry* **2010**, *49*, 1147–1150. [[CrossRef](#)]
24. Nomura, T.; Aida, M.; Shinomiya, K.; Hano, Y. Artonins J, K, and L, three new isoprenylated flavones from the root bark of *Artocarpus heterophyllus* Lamk. *Heterocycles* **1993**, *36*, 575–580. [[CrossRef](#)]
25. Ferrari, F.; Messana, I.; de Araujo, M. Three new flavone derivatives, brosimones G, H, and I, from *Brosimopsis oblongifolia*. *Planta Med.* **1989**, *55*, 70–72. [[CrossRef](#)] [[PubMed](#)]
26. Cao, S.; Butler, M.S.; Buss, A.D. Flavonoids from *Artocarpus lanceifolius*. *Nat. Prod. Lett.* **2003**, *17*, 79–81. [[CrossRef](#)] [[PubMed](#)]
27. Hakim, E.H.; Aimi, N.; Kitajima, M.; Takayama, H. Artoindonesianin P, a new prenylated flavone with cytotoxic activity from *Artocarpus lanceifolius*. *Fitoterapia* **2003**, *73*, 668–673. [[CrossRef](#)]
28. Suhartati, T.; Achmad, S.A.; Aimi, N.; Hakim, E.H.; Kitajima, M.; Takayama, H.; Takeya, K. Artoindonesianin L, a new prenylated flavone with cytotoxic activity from *Artocarpus rotunda*. *Fitoterapia* **2001**, *72*, 912–918. [[CrossRef](#)]
29. Jayasinghe, U.L.B.; Samarakoon, T.B.; Kumarihamy, B.M.M.; Hara, N.; Fujimoto, Y. Four new prenylated flavonoids and xanthenes from the root bark of *Artocarpus nobilis*. *Fitoterapia* **2008**, *79*, 37–41. [[CrossRef](#)]
30. Lin, C.N.; Shieh, W.L. Pyranoflavonoids from *Artocarpus communis*. *Phytochemistry* **1992**, *31*, 2922–2924.
31. Syah, Y.M.; Achmad, S.A.; Ghisalberti, E.L.; Hakim, E.H.; Makmur, L.; Mujahidin, D. Artoindonesianins Q–T, four isoprenylated flavones from *Artocarpus champeden* Spreng. *Phytochemistry* **2002**, *61*, 949–953. [[CrossRef](#)]
32. Nomura, T.; Aida, M.; Yamaguchi, N.; Hano, Y. Artonols A, B, C, D, and E, five new isoprenylated phenols from the bark of *Artocarpus communis* forst. *Heterocycles* **1997**, *45*, 163–175. [[CrossRef](#)]
33. Hakim, E.H.; Fahriyati, A.; Kau, M.S.; Achmad, S.A.; Makmur, L.; Ghisalberti, E.L.; Nomura, T. Artoindonesianins A and B, two new prenylated flavones from the root of *Artocarpus champeden*. *J. Nat. Prod.* **1999**, *62*, 613–615. [[CrossRef](#)] [[PubMed](#)]
34. Ko, F.N.; Cheng, Z.J.; Lin, C.N.; Teng, C.M. Scavenger and antioxidant properties of prenylflavones isolated from *Artocarpus heterophyllus*. *Free Radic. Biol. Med.* **1998**, *25*, 160–168. [[CrossRef](#)]
35. Widyawaruyanti, A.; Kalauni, S.K.; Awale, S.; Nindatu, M.; Zaini, N.C.; Syafruddin, D.; Asih, P.B.; Tezuka, Y.; Kadota, S. New prenylated flavones from *Artocarpus champeden*, and their antimalarial activity in vitro. *J. Nat. Med.* **2007**, *61*, 410–413. [[CrossRef](#)]

36. Wang, X.L.; Di, X.X.; Shen, T.; Wang, S.Q.; Wang, X.N. New phenolic compounds from the leaves of *Artocarpus heterophyllus*. *Chin. Chem. Lett.* **1998**, *28*, 37–40. [[CrossRef](#)]
37. Ramli, F.; Rahmani, M.; Kassim, N.K.; Hashim, N.M.; Sukari, M.A.; Akim, A.M.; Go, R. New diprenylated dihydrochalcones from leaves of *Artocarpus elasticus*. *Phytochem. Lett.* **2013**, *6*, 582–585. [[CrossRef](#)]
38. Aida, M.; Shinomiya, K.; Matsuzawa, K.; Hano, Y. Artonins Q, R, S, T, and U, five new isoprenylated phenols from the bark of *Artocarpus heterophyllus* Lamk. *Heterocycles* **1994**, *39*, 847–858.
39. Arung, E.; Shimizu, K.; Kondo, R. Inhibitory effect of isoprenoid-substituted flavonoids isolated from *Artocarpus heterophyllus* on Melanin biosynthesis. *Planta Med.* **2006**, *72*, 847–850. [[CrossRef](#)]
40. Wenkert, E.; Gottlieb, H.E. Carbon-13 nuclear magnetic resonance spectroscopy of flavonoid and isoflavonoid compounds. *Phytochemistry* **1977**, *16*, 1811–1816. [[CrossRef](#)]
41. Nomura, T.; Fukai, T.; Yamada, S.; Katayanagi, M. Studies on the constituents of the cultivated mulberry tree II. Photo-oxidative cyclization of morusin. *Chem. Pharm. Bull.* **1978**, *26*, 1431–1436. [[CrossRef](#)]
42. Chung, M.I.; Lu, C.M.; Huang, P.L.; Lin, C.N. Prenylflavonoids of *Artocarpus heterophyllus*. *Phytochemistry* **1995**, *40*, 1279–1282. [[CrossRef](#)]
43. Kijjoa, A.; Cidade, H.M.; Pinto, M.M.M.; Gonzalez, M.J. Prenylflavonoids from *Artocarpus elasticus*. *Phytochemistry* **1996**, *43*, 691–694. [[CrossRef](#)]
44. Nomura, T.; Hano, Y.; Inami, R. Components of the bark of *Artocarpus rigida* Bl. 1. structures of two new isoprenylated flavones, Artonins G and H. *Heterocycles* **1990**, *31*, 2173–2179. [[CrossRef](#)]
45. Rao, A.R.; Varadan, M.; Venkataraman, K. Coloring matters of wood of *Artocarpus heterophyllus*. 7. Isocycloheterophyllin, a new flavone. *Indian J. Chem.* **1973**, *11*, 298–299.
46. Syah, Y.M.; Achmad, S.A.; Ghisalberti, E.L.; Hakim, E.H.; Makmur, L.; Mujahidin, D. Artoindonesianins G-I, three new isoprenylated flavones from *Artocarpus lanceifolius*. *Fitoterapia* **2001**, *72*, 765–773. [[CrossRef](#)]
47. Dej-adisai, S.; Meechai, I.; Puripattanon, J.; Kummee, S. Antityrosinase and antimicrobial activities from Thai medicinal plants. *Arch. Pharm. Res.* **2013**, *37*, 473–483. [[CrossRef](#)]
48. Nomura, T.; Hano, Y.; Aida, M.; Shiina, M.; Kawai, T.; Ohe, H.; Kagei, K. Artonins A and B, two new prenylflavones from the root bark of *Artocarpus heterophyllus* Lamk. *Heterocycles* **1989**, *29*, 1447–1453. [[CrossRef](#)]
49. Fujimoto, T.; Hano, Y.; Nomura, T.; Uzawa, J. Components of root bark of *Cudrania tricuspidata* 2. structures of two new isoprenylated flavones, Cudraflavones A and B. *Planta Med.* **1984**, *50*, 161–163. [[CrossRef](#)]
50. Septama, A.W.; Panichayupakaranant, P. Antibacterial assay-guided isolation of active compounds from *Artocarpus heterophyllus* heartwoods. *Pharm. Biol.* **2015**, *53*, 1–6. [[CrossRef](#)]

Sample Availability: Samples of the compounds (PFs 1–15) are available from the authors.



© 2019 by the authors. Licensee MDPI, Basel, Switzerland. This article is an open access article distributed under the terms and conditions of the Creative Commons Attribution (CC BY) license (<http://creativecommons.org/licenses/by/4.0/>).